Supplemental material: Label-free imaging of female genital tract melanocytic lesions with pump-probe microscopy: A promising diagnostic tool

Francisco E. Robles, Sanghamitra Deb, Martin C. Fischer, Warren S. Warren*, M. Angelica Selim

* Corresponding author: warren.warren@duke.edu

Supplemental Methods

Pump-probe system and data acquisition

The pump-probe system (Fig. S1) has been described in detail elsewhere[1-3]. In short, we integrated a commercial laser-scanning microscope (Zeiss, LSM 510) with a custom laser setup that produces two ultrafast pulse trains (~125 fs pulses each, with an 80 MHz repetition rate) tuned to 730 nm (pump) and 810 nm (probe). This wavelength combination produces drastically different transient responses for various types of melanins[4]. The pump pulse train is amplitude-modulated at 4.5 MHz using an acousto-optic modulator (AOM), and the relative time delay between the pump and probe pulses is adjusted using a delay stage. Then the two beams are spatially overlapped and sent collinearly to the laser-scanning microscope. The pulses are focused onto the sample using a 20X objective (0.8NA) with less than 0.65 mW total power to avoid any effects that may alter the melanin pigment chemistry (e.g., photobleaching)[4]. At the focus, the two beams interact with the sample. Then, the pump is then removed from the transmitted light using a dichroic filter and the remaining probe light is collected using a photodiode. The nonlinear signal (based on transferred modulation from the pump to the probe due to the nonlinear interaction) is detected using a custom-built lock-in amplifier with a time constant of ~5 μs. To measure the transient dynamics, we acquire multiple images at the same location (420 μm x 420 μm field of view), each with a different pump-probe time-delay. A stack of 22 images is collected, with pump-probe time-delays ranging from -1.5 ps (i.e., probe precedes the pump) to 3 ps. Acquisition time per stack is ~6 minutes. A total of 612 pump-probe stacks were acquired.

Quantification of pigment structure

To quantify the image structure we used a 2-dimensional mathematical autocorrelation transformation: For each gray-scale image, we compute a two-dimensional autocorrelation (AC) and compute the 2-dimensional distribution anisotropy, AC entropy, and estimate of the image signal to noise ratio (used as a metric of degree of pigmentation, since the noise is adjusted to a constant level) [1,5]. This transformation, also known as a morphological autocorrelation transformation, provides insight into the morphological covariance, and the parameters derived from it are invariant to translation, scale, and rotation [6]. We also compute the cross-correlation (XC) between the two gray scale images with biochemical information, and extract the same parameters which serve as additional indicators of degree of chemical and spatial heterogeneity. For more details see Refs.[1,5].

Statistical analysis

A total of 30 parameters were extracted for each pump-probe image stack. These include the average and standard deviation of θ; mean and standard deviation of the three PCs, normalized by the total signal intensity; entropy of the spherical coordinates (R, θ and φ); the variance accounted for by the top 3 PCs of each individual image; and the SNR, anisotropy and entropy of the gray-scale images (based on AC and XC). Border areas (e.g., a single 420 µm X 420 µm image containing both normal tissue and melanoma regions) were not included in the quantitative analysis that determines the predictive power.

The following statistical analysis is used to reduce the number of parameters and assess the predictive power of the method [1]: First, we apply forward sequential feature selection in a wrapper fashion (using a nested 10-fold cross validation) [7] with data drawn from individual images to maximize the variance of the data. This process reduces the number of parameters from 30 to 7 or 4, depending on the specific test (e.g., melanomas vs. non-melanomas, or non-metastatic melanomas vs. metastatic melanomas), and allows us to elucidate which image features are the most diagnostically relevant. Finally, using the selected parameters, we test the method's predictive power using the leave one out cross validation (LOOCV) method, with each specimen (i.e., all images from a single specimen) treated as the test set, and the remaining used for training. Thus, for each iteration, the test set is completely independent

from the training set. Classification is based on support vector machine learning using a Gaussian radial basis function kernel.

Preliminary statistical analysis

Using the seven selected parameters, we constructed a confusion matrix which allows us to gain a general sense of how well each type of lesion can be differentiated from all of the others (the model is tested using 10-fold cross validation; Fig S2). Here normal regions were omitted due to the small sample size in this category, and all melanomas (in-situ and invasive) were grouped together since both lead to surgical treatments. The results show that each lesion can be uniquely identified with high specificity and low false negative rates (overall sensitivity and specificity for identifying melanoma is 94% and 79%, respectively). The highest false negative rate (FNR = 26%) was between melanotic macules and melanomas, suggesting these lesions are the most difficult to identify with these parameters. For comparison, Fig. S2B show the confusion matrix of the same data but using a model that is based on only the structural parameters (see Fig. 5). The results exhibit much lower sensitivity and higher false negative rates compared to the optimized parameters. The overall sensitivity for melanoma was 92% and specificity 27%. These results indicate that the biochemical information is critical for improving the specificity towards disease.

While the confusion matrix allows us to get a sense of how well the method can differentiate between lesion types, the approach is overly optimistic for assessing the overall predictive power, as it treats each *image* as independent. To more accurately estimate the predictive power of pump-probe microscopy, we use the leave one out cross validation (LOOCV) method with individual *lesions* (i.e., all images from a patient) used as the test set and all others as the training set. This is described in detail in the results section of the main text

Does the fixation process alter the melanin pump-probe signal?

We conducted several tests to identify any possible changes in the melanin signals resulting from processing the samples. Using black hairs, we tested how leaving the samples in formalin for different amounts of time (1, 4, 8, 12, 24 hrs) may alter the signals. Results do not show any significant changes on the pump-probe melanin signals (data not shown). Using pigmented tissue (normal), we compared fixed and unfixed samples, which also did not show any differences. We also conducted tests using b16 cells live

and fixed with different methods of fixation, including formalin, methanol, and ethanol. No significant changes were observed. We have also imaged eumelanin derived from a Jurassic cephalopod[8]. Results show that signals from the fossil are essentially identical to that of eumelanin extracted from its modern-day counterpart, Sepia officinalis[8]. These are also similar to signals from human tissue specimens[1,3]. Thus, there is no evidence that either the fixation or storing of the samples alters the melanin pump-probe signals.
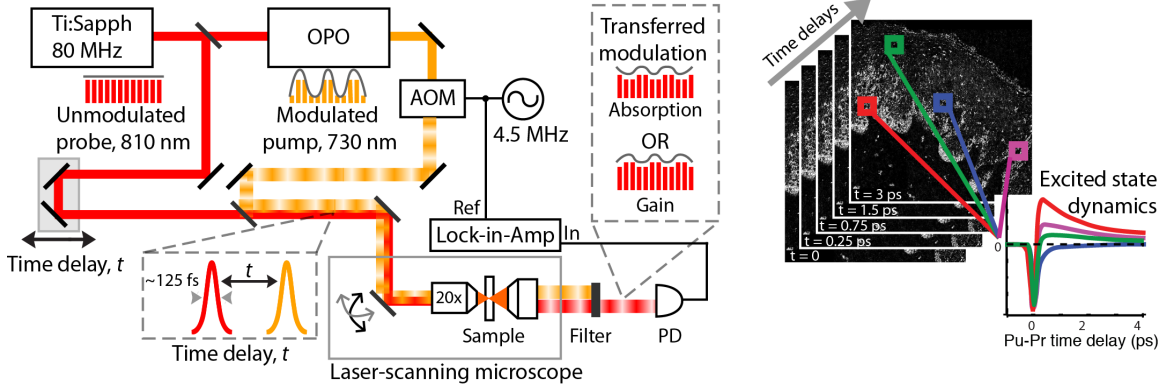
Supplemental Figures:

Figure S1: System schematic and data acquisition. Ti:Sapph: Titanium-Sapphire laser. OPO: Optical Parametric Oscillator. AOM: Acousto-Optic Modulator. PD: Photodiode.
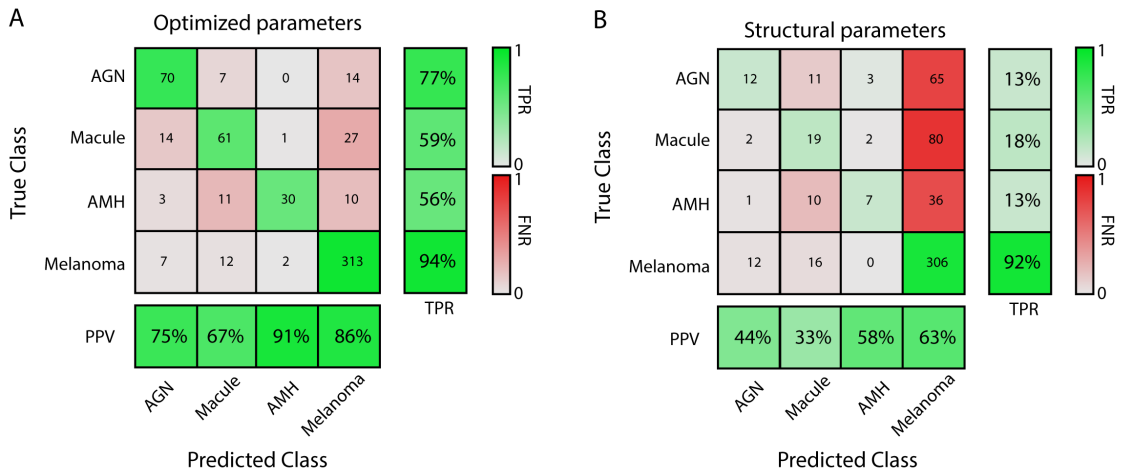

Figure S2: Confusion matrix using optimized parameters (A) and structural parameters (B)

References

1. Robles, F. E. *et al.* Pump-probe imaging of pigmented cutaneous melanoma primary lesions gives insight into metastatic potential. *Biomedical Optics Express* **6,** 3631–3645 (2015).

2. Fu, D., Ye, T., Matthews, T. E., Yurtsever, G. & Warren, W. S. Two-color, two-photon, and excited-state absorption microscopy. *J Biomed Opt* **12,** 054004 (2007).

3. Matthews, T. E., Piletic, I. R., Selim, M. A., Simpson, M. J. & Warren, W. S. Pump-probe imaging differentiates melanoma from melanocytic nevi. *Science Translational Medicine* (2011). doi:10.1126/scitranslmed.3001604

4. Simpson, M. J. *et al.* Near-Infrared Excited State Dynamics of Melanins: The Effects of Iron Content, Photo-Damage, Chemical Oxidation, and Aggregate Size. *J. Phys. Chem. A* **118,** 993–1003 (2014).

5. Robles, F. E., Wilson, J. W. & Warren, W. S. Quantifying melanin spatial distribution using pump-probe microscopy and a 2-D morphological autocorrelation transformation for melanoma diagnosis. *J Biomed Opt* **18,** 120502 (2013).

6. Loui, A. P. A., Venetsanopoulos, A. N. A. & Smith, K. C. K. Morphological autocorrelation transform: A new representation and classification scheme for two-dimensional images. *IEEE Trans Image Process* **1,** 337–354 (1992).

7. Aha, D. W. & Bankert, R. L. in *Learning from Data* **112,** 199–206 (Springer New York, 1996).

8. Simpson, M. J. *et al.* Pump–Probe Microscopic Imaging of Jurassic-Aged Eumelanin. *J. Phys. Chem. Lett.* **4,** 1924–1927 (2013).